Structural Engineering and Mechanics, *Vol. 75, No. 5 (2020) 559-569*
DOI: https://doi.org/10.12989/sem.2020.75.5.559

Out-of-plane ductile failure of notch: Evaluation of Equivalent Material Concept

A. R. Torabi [1a], Behnam Saboori [*2] and M. R. Kamjoo [1b]

[1] *Fracture Research Laboratory, Faculty of New Sciences and Technologies, University of Tehran, P.O. Box 14395-1561, Tehran, Iran*
[2] *Fatigue and Fracture Research Laboratory, Center of Excellence in Experimental Solid Mechanics and Dynamics, School of Mechanical Engineering, Iran University of Science and Technology, Narmak, 16846 Tehran, Iran*

(Received July 8, 2019, Revised October 1, 2020, Accepted March 15, 2020)

Abstract. In the present study, the fracture toughness of U-shaped notches made of aluminum alloy Al7075-T6 under combined tension/out-of-plane shear loading conditions (mixed mode I/III) is studied by theoretical and experimental methods. In the experimental part, U-notched test samples are loaded using a previously developed fixture under mixed mode I/III loading and their load-carrying capacity (LCC) is measured. Then, due to the presence of considerable plasticity in the notch vicinity at crack initiation instance, using the Equivalent Material Concept (EMC) and with the help of the point stress (PS) and mean stress (MS) brittle failure criteria, the LCC of the tested samples is predicted theoretically. The EMC equates a ductile material with a virtual brittle material in order to avoid performing elastic-plastic analysis. Because of the very good match between the EMC-PS and EMC-MS combined criteria with the experimental results, the use of the combination of the criteria with EMC is recommended for designing U-notched aluminum plates in engineering structures. Meanwhile, because of nearly the same accuracy of the two criteria and the simplicity of the PS criterion relations, the use of EMC-PS failure model in design of notched Al7075-T6 components is superior to the EMC-MS criterion.

Keywords: fracture toughness; U-shaped notch; ductile failure; Equivalent Material Concept; mixed mode I/III loading

1. Introduction

In design of many engineering components, various notches such as V- and U-shaped ones are used to locate parts in the main structure and connect them to other components or for other applications. These notches, depending on their geometry, have high stress concentrations around their borders and reduce the load-carrying capacity (LCC) of engineering parts. Therefore, investigating the phenomenon of notch fracture is necessary and of great importance, and many researchers have dealt with the problem by using diverse methods (El Minor *et al.* 2007; Lee 2010; Lee *et al.* 2016; Haeri *et al.* 2018; Sarfarazi *et al.* 2019; Gómez *et al.* 2007, 2008, 2009).

In general, the fracture behavior of material can be classified as ductile and brittle. Brittle fracture occurs very quickly and together with unstable crack growth. Since brittle fracture is sudden and can cause severe damage, brittle components are not usually used in engineering structures for the purpose of load bearing. Conversely, ductile fracture occurs slowly after moderate or large plastic deformations for which the crack growth is normally stable. The slow growth of cracks in ductile materials makes it easy to detect crack growth during periodic inspections. Some metals and alloys, including aluminum alloys, show ductile behavior in a wide range of working temperatures.

Because of the widespread application of ductile materials, e.g. steels, aluminum alloys, and a large group of polymers, etc., in engineering structures, it is essential to examine the LCC of notched ductile parts under various loading conditions. Since ductile fracture in notched parts due to stress concentration is associated with significant plastic deformations in the vicinity of notch edge, the linear elastic fracture criteria cannot be used to predict the failure behavior of notched ductile materials. In these cases, it is necessary to apply the criteria of the elastic-plastic fracture mechanics, such as the J-integral, the crack tip opening displacement (CTOD), and so on. On the other hand, the ductile fracture criteria are time-consuming to be applied because of the need for complex elastic-plastic analyses. In order to avoid these complexities, Torabi (2012a) presented a new concept, named as the Equivalent Material Concept (EMC) in 2012. On the basis of this concept, the tensile strain energy density (i.e. the area under the stress-strain curve of uniaxial tension) of a ductile material until necking is assumed to be equivalent to that of a virtual brittle material with the same elastic modulus. It is noteworthy that the EMC seems to be similar to the Glinka's (Glinka 1985; Molski and Glinka 1981) equivalent strain energy density (ESED) concept, but there is a main difference between these two concepts. In accordance with the ESED, the stresses and strains near notches in inelastic materials are obtained while the purpose of the EMC is to determine the tensile strength of the equivalent material. The EMC combined with some brittle fracture criteria, such as the mean stress (MS) and point stress (PS) criteria, has already been found successful in predicting ductile fracture under combined *tension/in-plane shear* loading (mixed mode I/II)

*Corresponding author, Ph.D.
E-mail: b_saboori@alumni.iust.ac.ir
[a] Associate Professor
[b] M.Sc.

ISSN: 1225-4568 (Print), 1598-6217 (Online)

conditions. It is worth mentioning that for ductile materials with simultaneously significant strain-hardening and strain-to-failure, EMC seems to be null in predicting the failure load of notched components. For such materials, Torabi and Kamyab (2019a, b) presented the Fictitious Material Concept (FMC) by which fictitious values of Young's modulus and fracture toughness are defined and calculated for the real ductile material to predict LCC of notched specimens.

By comparing the tensile LCC of the V-notched ductile materials estimated by EMC-MS with the corresponding test results, Torabi (2012a) showed that the predictions derived from the MS criterion and EMC combination have a good accuracy. Torabi (2012b) also examined the LCC of ductile steel screws containing V-shaped threads subjected to pure mode I loading by using the EMC-MS criterion. In that research, he used two different types of steel with different mechanical properties and evaluated the LCC of the screws. The results implied a very good consistency between the experimental and theoretical results. In 2013, Torabi (2013) investigated the LCC of U-notched steel samples under the regime of large-scale yielding (LSY) utilizing the EMC. The investigation showed an acceptable difference between the experimental results and the predicted values, and therefore, the EMC efficiency was again approved. Torabi and Habibi (2016), in 2016, assessed the LCC of Al6061-T6 plates containing U-shaped notches under the in-plane mixed mode loading conditions. In view of the remarkable plastic deformation of Al6061-T6, they utilized the combination of EMC and brittle fracture criteria to predict the LCC of the test specimens. By comparing the theoretical and experimental results, they found that the use of the EMC was successful. Torabi and Alaei studied the LCC of the Al7075-T6 plates containing a V-notch subjected to mixed mode I/II loading (Torabi and Alaei 2015), and subjected to pure mode I loading (Torabi and Alaei 2016). They employed the EMC combined with two fracture criteria of MS and maximum tangential stress (MTS) or PS to predict the LCC of the aluminum test specimens. By comparing theoretical and experimental results, it was clear that the predictions of both the EMC-MTS and EMC-MS criteria were precise enough. Torabi and Keshavarzian (2016), in 2016, examined the LCC of the V-notched Al6061-T6 plates under mixed mode I/II loading. Their observations revealed that the size of the plastic region around the notch tip is large and the ductile failure regime is LSY. By comparing the experimental and theoretical results in that study, it was found that although both the EMC-MTS and EMC-MS criteria are suitable for predicting the LCC of the notched components, the EMC-MS criterion is relatively more precise than the EMC-MTS one. Torabi et al. (2016b), in 2016, estimated the LCC of the V-notched Al6061-T6 plates under mixed mode I/II loading using the EMC in combination with the averaged strain energy density (ASED) criterion and achieved successful results. The ASED criterion alone has been successful in the assessment of the brittle fracture of notched components (Torabi and Berto 2014; Saboori, Torabi, Berto, *et al.* 2018; Gómez *et al.* 2007). Torabi et al. (Torabi *et al.* 2016a) also predicted the LCC of the Al7075-T6 specimens weakened by a V-shaped notch under mixed mode I/II loading well in 2016. They found that the specimens failed by LSY regime. Torabi, Campagnolo, et al. (2017), in 2017, explored the LCC of the V-notched Al6061-T6 plates under pure mode I loading, and reported that the result of the EMC-ASED criterion is also satisfactory in that problem. In 2017, the LCC of the Al6061-T6 samples weakened by V-notches subjected to the mixed mode I/II loading case was also successfully assessed by Torabi, Berto, et al. (2017) using the EMC-ASED criterion. Torabi, Berto, et al. (2018), studied the failure of the V-notched Al7075-T6 plates under in-plane mixed mode loading and found good results in utilizing the EMC. In 2017, Torabi and Mohammad Hosseini (2017) studied the LCC of the U-notched Al7075-T6 plates under mixed mode I/II loading with high accuracy by applying the EMC to one of the brittle fracture criteria. The EMC has also been coupled with the failure model of Finite Fracture Mechanics (FFM) to study the fracture of notched metallic elements (Sapora and Firrao 2017; Torabi *et al.* 2019). Some other contributions regarding the role of EMC in successful failure prediction of notched ductile specimens under *in-plane loading conditions* can also be found in literature (see for instance (Cicero *et al.* 2018; Torabi and Kamyab 2019c; Fuentes *et al.* 2018; Torabi, Rahimi*, et al.* 2018)).

As seen above, all the ductile fracture studies, done so far with the aid of EMC on the notched elements, are limited to the loading conditions of pure mode I and in-plane mixed mode (mixed mode I/II). In order to evaluate the effectiveness of EMC in other loading conditions, in this study, by combining this concept with two brittle fracture criteria of PS and MS, the fracture toughness of U-notched Al7075-T6 plates under out-of-plane mixed mode I/III loading is estimated. In addition, 21 U-notched test specimens are made of Al7075-T6 and subjected to different mixed mode I/III loading conditions until fracture using a previously developed loading fixture. Thereafter, the notch fracture toughness values estimated by the EMC-PS and EMC-MS criteria are successfully verified by comparing them with the results of the fracture tests.

2. Fracture tests of U-notched Al7075-T6 specimens

In this section, a new set of mixed mode I/III fracture tests conducted on U-notched plates made from Al7075-T6 is described in detail. In Fig. 1, the geometry and dimensional details of a rectangular test sample containing a U-notch is shown. In order to experimentally investigate the effect of notch tip radius on fracture behavior of the test samples, two notch tip radii of 1 and 2 mm are considered in the tests.

As mentioned earlier, aluminum alloy Al7075-T6 is used to fabricate the samples. This alloy has many industrial applications and is exploited extensively in aerospace structures.

To obtain a number of material properties of the utilized alloy, tensile tests are carried out in accordance with the ASTM E8 (2016) standard. The obtained true and

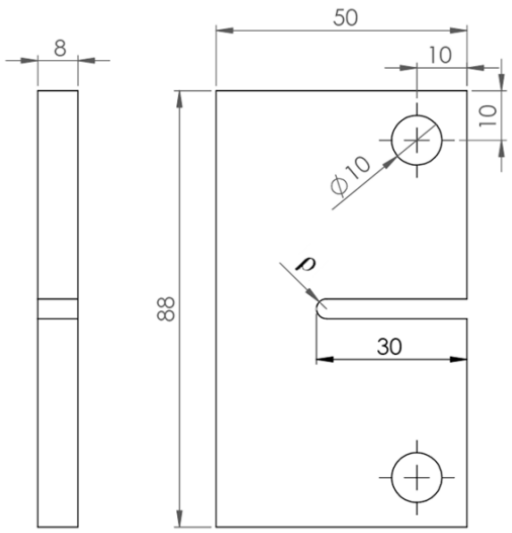

Fig. 1 U-notched rectangular test specimen (dimensions in mm)

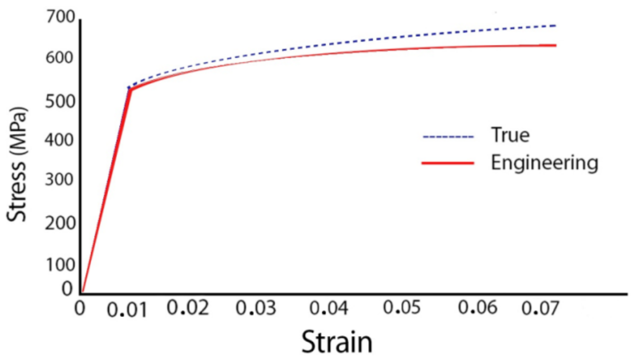

Fig. 2 True and engineering stress-strain curves obtained for Al 7075-T6

Table 1 Mechanical properties experimentally obtained for Al 7075-T6

Material Property	Value
Elastic modulus, E [GPa]	72
Poisson's Ratio, v	0.33
Tensile yield strength [MPa]	547
Ultimate Tensile Strength [MPa]	612.5
Engineering strain at maximum load	0.07
True fracture stress [MPa]	1.96
Fracture toughness, K_c [MPa√m]	45.62

engineering stress-strain curves are represented in Fig. 2. Moreover, Table 1 lists the values of the mechanical properties of the Al7075-T6 alloy. The fracture toughness value is determined according to ASTM B646-19 (2019).

To prepare the specimens required for the fracture tests, an Al7075-T6 plate with a thickness of 8 mm is first provided and then, using a water-jet cutting machine, the desired samples are cut from the plate. In Fig. 3, the U-notched samples with the notch tip radii of 1 mm and 2 mm are depicted.

Fig. 3 The provided U-notched test specimens with notch tip radii of 1 and 2 mm

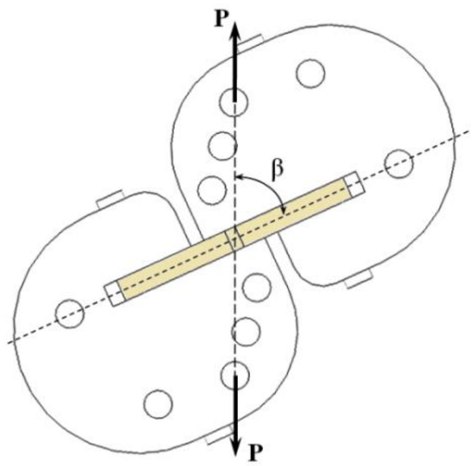

Fig. 4 Schematic of the loading fixture used for mixed-mode I/III fracture experiments

To exert different mixed mode I/III loading conditions, the test specimens are fastened with two pairs of bolts and nuts on the loading fixture shown in Fig. 4, and the fixture is assembled by two Y-shaped intermediate pieces in a uniaxial tensile testing device. This fixture has already been successfully employed to explore the fracture behavior of cracked (Ayatollahi and Saboori 2015), U-notched (Saboori *et al.* 2017; Torabi and Saboori 2018) and V-notched (Saboori, Torabi and Keshavarz Mohammadian 2018; Torabi, Saboori, *et al.* 2018) components.

This fixture, by changing the attitude of the test sample relative to the direction of the test apparatus loading axis, causes various load combinations to be applied to the specimen. The angle β corresponding to each of the holes embedded in the loading fixture is shown in Fig. 4, which represents various combinational loading modes. The angle β can be 0°, 40°, 65°, 72° or 90°, where β = 0° corresponds to the pure mode I loading, β = 90° corresponds to the loading under pure mode III, and each of the other angles corresponds to a certain combination of mode I and mode III loadings. In the present study, for each notched specimen with 1 or 2 mm tip radius, in addition to the pure mode I fracture test, several mixed mode I/III experiments are also performed. Considering at least 3 replicas of each test to verify the repeatability of the results, ultimately, 21 samples are prepared for the tests.

Fig. 5 The test specimen and loading fixture during one of the fracture tests

Fig. 6 Notched test specimen with ρ = 2 mm broken under mixed-mode I/III loading

In Fig. 5, an image of the loading fixture and the test sample during the fracture test is observed. The tests are carried out under the displacement-control conditions at a speed of 3 mm/min satisfying the quasi-static loading conditions.

Fig. 6 displays a broken test sample. The load-displacement diagrams obtained demonstrate that the Al7075-T6 specimens have elastic-plastic behavior. The load-displacement diagram for one of the tested U-notched samples is shown in Fig. 7.

Interesting in testing the fracture of the specimens is their sudden failure, despite the presence of considerable plasticity near the notch edge. This phenomenon results from a very small distance between the ultimate and final rupture points in the tensile stress-strain curve (see Fig. 2). Such a sudden fracture behavior has also been reported in the past for Al7075-T6 under mixed mode I/II loading (see for example (Torabi *et al.* 2016b) and (Torabi, Berto*, et al.* 2018)). In other words, observations during the tests indicate that significant plastic deformations around the notch tip do not guarantee the stability of crack growth and rupture of parts made of ductile materials. The behavior of cracking and crack extension in ductile materials can be justified using the engineering stress-strain curve of the materials. In spite of the strain until failure, which is usually a large amount for ductile materials, the strain corresponding to the ultimate point is a key parameter in understanding the behavior of cracking and crack extension in this category of materials. The small difference between the strains of the ultimate and final rupture points, as seen in Fig. 2 for Al7075-T6 alloy, means that the cracks in the material nucleate in exchange for large plastic deformations and the material breaks suddenly due to the unstable crack growth. On the contrary, if the ultimate strain forms a small fraction of the total strain that leads to the material rupture, cracking happens rapidly by relatively small plastic deformations and the crack spreads slowly through large plastic deformations up to final rupture. This last statement has been reported in Refs. (Torabi and Habibi 2016) and (Torabi and Alaei 2016)for Al6061-T6 specimens weakened by U- and V-notches and subjected to in-plane loading conditions.

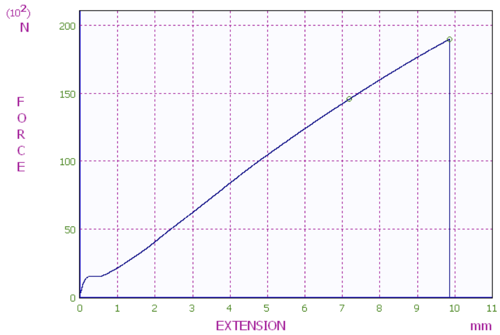

Fig. 7 Load-displacement curve of the test sample with ρ = 2 mm broken under the loading case of $\beta = 65^\circ$

Table 2 Load-carrying capacity of the U-notched Al7075-T6 samples

Specimen index	P_1 (N)	P_2 (N)	P_3 (N)	P_{avg} (N)
U-1-0	16220	16330	15793	16536
U-1-40	14559	14093	14630	14954
U-1-65	12841	13335	12419	12769
U-1-72	13533	13696	13118	13784
U-2-0	18639	18640	18809	18467
U-2-40	18390	18037	19711	17423
U-2-65	18226	18000	18603	18074

The load-displacement curves obtained specify the LCC values of the U-notched samples. In Table 2, the LCCs of these specimens are presented under different loading modes corresponding to $\beta = 0^\circ$, 40°, 65°, and 72° for the notch tip radius of 1 and $\beta = 0^\circ$, 40° and 65° for the notch tip radius of 2 mm. The values shown in this table as P_{avg} are the average fracture load of the three replicates of each test. Each specimen in Table 2 is denoted by a specific index X-Y-Z, in which X, Y, and Z correspond to the notch shape, the notch tip radius, and the β angle, respectively. For example, the sample with U-1-40 index corresponds a U-notched specimen with a tip radius of 1 mm, which is loaded under mixed mode I/III conditions associated with the angle $\beta = 40^\circ$ in the loading fixture.

3. Point stress and mean stress criteria

3.1 Point stress (PS) criterion

Fig. 8 displays the schematic of a round-tip V-shaped notch and the coordinate systems defined for it.

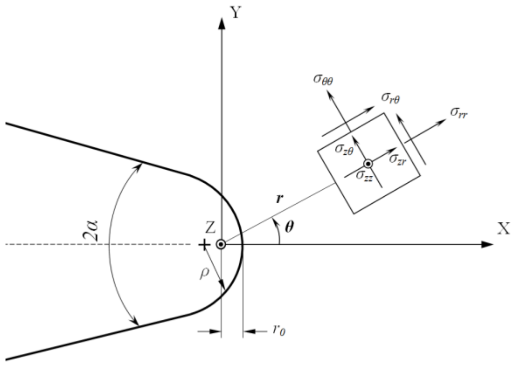

Fig. 8 Typical round-tip V-notch

In 2010, Ayatollahi and Torabi (2010b) extended the well-known MTS criterion (Erdogan and Sih 1963) proposed for cracked pieces to the parts weakened by round-tip V-notches and provided a new criterion, known as RV-MTS or point stress (PS), for predicting their brittle fracture. Based on this criterion, brittle fracture of a V-notched component occurs when the tangential stress at a specific critical radial distance, r_c, from the notch edge (or critical radial distance from the origin of the polar coordinate system, $r_{c,V}$) reaches the critical stress of material, σ_c. The indicated critical distance is considered to be a material property. The critical stress σ_c is also considered to be a material property and is independent of geometry and loading conditions. This parameter is taken into consideration to be equal to the tensile strength for brittle and quasi-brittle materials, because the final failure for a specimen under tensile loading occurs only when the inter-molecular bonding of the substance is broken down. Another assumption of the PS criterion is that fracture begins from a point on the notch edge, radially and along the direction perpendicular to the maximum tangential stress.

Recently, the formulation of the PS criterion for the fracture of V-notches under the general loading of mixed mode I/II/III has been presented (Saboori *et al.* 2016). Given that a U-notch is equivalent to a V-shaped notch with the opening angle of 2α = 0°, the proposed formulation can be used to study the failure of U-notched parts. The prediction of the PS criterion for the fracture limit of U-notched parts under mixed mode I/III loading can be depicted in the form of the curves of $K_{III}^{U,\rho}/K_{Ic}^{U,\rho}$ versus $K_I^{U,\rho}/K_{Ic}^{U,\rho}$. The parameters $K_I^{U,\rho}$ and $K_{III}^{U,\rho}$ are the mode I and mode III notch stress intensity factors (NSIFs) and $K_{Ic}^{U,\rho}$ is the mode I notch fracture toughness, which has a different magnitude for each radius of the notch tip. Based on the PS criterion, the normalized NSIFs of $K_{III}^{U,\rho}/K_{Ic}^{U,\rho}$ and $K_I^{U,\rho}/K_{Ic}^{U,\rho}$ as well as the out-of-plane fracture angle of the notched member, ϕ_f, for each combination of loading modes are obtained from the simultaneous solution of the following equations (Saboori *et al.* 2016):

$$\frac{K_I^{U,\rho}}{r_{c,U}{}^S}\left[\nu\left(L(A+R)+M\left(\frac{r_{c,U}}{r_0}\right)^P(B+V)\chi_{d1}\right)-L(R+S\chi_{b1})-M\left(\frac{r_{c,U}}{r_0}\right)^P(\chi_{c1}+V\chi_{d1})\right]sin2\phi_f-\frac{2K_{III}^{U,\rho}}{r_{c,U}{}^K}\left[1+\left(\frac{r_{c,U}}{r_3}\right)^Z\right]cos2\phi_f=0 \tag{1}$$

$$\begin{aligned}\frac{K_I^{U,\rho}}{K_{Ic}^{U,\rho}}&\left[L(R+S\chi_{b1})+M\left(\frac{r_{c,U}}{r_0}\right)^P(\chi_{c1}+V\chi_{d1})\right]cos^2\phi_f\\&-\frac{K_{III}^{U,\rho}}{K_{Ic}^{U,\rho}}\left[1+\left(\frac{r_{c,U}}{r_3}\right)^Z\right]sin2\phi_f\\&+\nu\frac{K_I^{U,\rho}}{K_{Ic}^{U,\rho}}\left[L(A+R)\right.\\&\left.+M\left(\frac{r_{c,U}}{r_0}\right)^P(B+V)\chi_{d1}\right]sin^2\phi_f\\&=L(R+S\chi_{b1})\\&+M\left(\frac{r_{c,U}}{r_0}\right)^P(\chi_{c1}+V\chi_{d1})\end{aligned} \tag{2}$$

Except $K_I^{U,\rho}$, $K_{III}^{U,\rho}$, $K_{Ic}^{U,\rho}$, r_0, $r_{c,U}$, ν and ϕ_f, the other parameters of Eqs. (1) and (2) are the constant coefficients dependent on the notch opening angle (with the value of zero for a U-notch). The values of those coefficients can be found in Ref. (Saboori *et al.* 2016). $r_{c,U}$ is the critical radial distance from the origin of the polar coordinate system of U-notch. The $r_{c,U}$ distance is correlated with r_c (the critical distance from the notch tip) via the following relation:

$$r_{c,U}=r_0+r_c \tag{3}$$

The critical distance r_c for brittle and quasi-brittle materials can be determined by the next equation (Susmel and Taylor 2008).

$$r_c=\frac{1}{2\pi}\left(\frac{K_{Ic}}{\sigma_u}\right)^2 \tag{4}$$

In the equation above, K_{Ic} is the plain-strain mode I fracture toughness and σ_u is the ultimate tensile strength of material.

3.2 Mean stress (MS) criterion

Ayatollahi and Torabi (2010a), based on the MS criterion provided by Wieghardt (1995) for cracked pieces, proposed a new fracture criterion for the members containing blunt V-notches subjected to mode I loading, in 2010. Based on this criterion, known as RV-MS or MS, brittle fracture happens in a loaded V-notched component, when the average tensile tangential stress at a specific critical distance, d_c, from the notch tip (or the critical radial distance from the origin of the polar coordinate system, $d_{c,V}$) reaches its critical value, σ_c. The critical distance in the MS criterion is also taken into account as one of the material properties.

Similar to the PS criterion, the MS criterion has already been formulated for fracture study of V-shaped notches under the general loading of mixed mode I/II/III (Saboori *et al.* 2016). According to the generalized MS criterion, the dimensionless normalized NSIFs of $K_{III}^{U,\rho}/K_{Ic}^{U,\rho}$ versus $K_{I}^{U,\rho}/K_{Ic}^{U,\rho}$ as well as the out-of-plane fracture angle of ϕ_f for each loading mode mixity are calculated by solving the following equations simultaneously (Saboori *et al.* 2016):

$$K_I^{U,\rho}(\nu C^* - A^*)\, sin2\phi_f + 2K_{III}^{U,\rho}\, B^*\, cos2\phi_f = 0 \tag{5}$$

$$\frac{K_I^{U,\rho}}{K_{Ic}^{U,\rho}} A^* cos^2\phi_f + \frac{K_{III}^{U,\rho}}{K_{Ic}^{U,\rho}} B^* sin2\phi_f + \nu \frac{K_I^{U,\rho}}{K_{Ic}^{U,\rho}} C^* sin^2\phi_f = A^* \tag{6}$$

Ref. (Saboori *et al.* 2016) has provided the equations calculating the constant parameters A^*, B^*, and C^* in terms of the notch characteristics. The critical distance measured from the origin of the U-notch polar coordinate system is determined from the following equation:

$$d_{c,U} = r_0 + d_c \tag{7}$$

where d_c stands for the critical distance measured from the notch tip. The following relation has been presented to specify d_c for brittle and quasi-brittle materials (Seweryn 1994):

$$d_c = \frac{2}{\pi}\left(\frac{K_{Ic}}{\sigma_u}\right)^2 = 4r_c \tag{8}$$

4. The equivalent material concept

As previously stated, a new concept, called the Equivalent Material Concept (EMC), has been presented to overcome the complexities of the elastic-plastic analysis required in the study of ductile fracture (Torabi 2012a). According to this concept, a ductile material can be assumed equivalent to a virtual brittle material, if their modulus of elasticity (E) and their strain energy density (SED) until the ultimate point of the tensile stress-strain curve of the ductile material are the same. SED is actually the strain energy absorbed by a material per unit volume. Accordingly, instead of using complex and time-consuming elastic-plastic analysis, linear elastic analysis can be used, and by combining the EMC with one of the brittle fracture criteria, ductile notch fracture can be estimated.

4.1 Tensile strength of the equivalent material

Torabi and Alaei (2016) applied the power-law stress-strain relation to the plastic zone of the ductile metallic material and by utilizing EMC, derived the following equation for calculating the tensile strength of the equivalent brittle material:

$$\sigma_f^* = \sqrt{{\sigma_Y}^2 + \frac{2Ek}{n+1}\left({\varepsilon_{u,true}}^{n+1} - 0.002^{n+1}\right)} \tag{9}$$

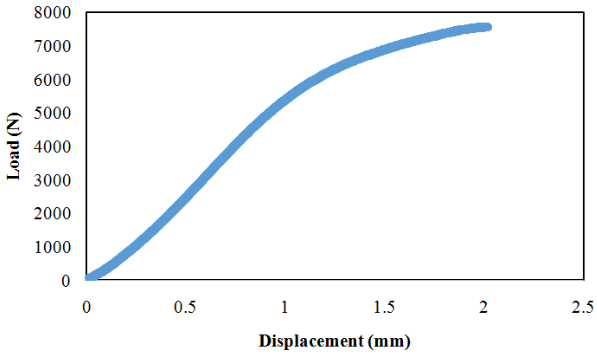

Fig. 9 Load-displacement curve of a ductile cracked specimen

where the parameters n, k, E, $\varepsilon_{u,true}$, and σ_Y are the strain-hardening exponent, the strain-hardening coefficient, the elastic modulus, the true plastic strain at the ultimate point, and the yield strength, respectively. Note that it is also possible to simply calculate the tensile strength of the equivalent material without using any equations for the stress-strain curve of the ductile material, e.g. the power-law equation etc. This can be done by directly computing the area under the stress-strain curve of ductile material until the ultimate point numerically and setting it equal to the area under the linear stress-strain curve of the equivalent material (see for instance Ref. (Torabi, Kalantari, *et al.* 2018)).

4.2 Fracture toughness of the equivalent material

As previously mentioned, in the estimation of brittle fracture using the PS and MS criteria, it is necessary to calculate the critical distance measured from the notch tip, r_c, by using Eq. (4). To analyze ductile fracture, the ductile material is assumed equivalent to a virtual brittle material, and in this sense, K_{Ic} (mode I fracture toughness) should be replaced with K_{Ic}^* (equivalent fracture toughness) and σ_u with σ_f^* (equivalent tensile strength). Therefore, in examining ductile fracture, Eq. (4) varies as follows:

$$r_c = \frac{1}{2\pi}\left(\frac{K_{Ic}^*}{\sigma_f^*}\right)^2 \tag{10}$$

To calculate the value of K_{Ic}^*, a commercial finite element (FE) software can be used. First, a FE model of the configuration of the cracked specimen fracture test is created in the software, and after applying the cracked sample LCC to that model and performing the stress analysis, the value of K_{Ic}^* is directly achieved.

In Fig. 9, a sample load-displacement diagram is shown for a cracked ductile component. In this figure, the area below the load-displacement diagram indicates the work required for the crack growth, and the peak of this graph specifies the LCC of the test specimen. In order to obtain the fracture toughness of the equivalent brittle material, it is necessary to calculate the area below the load-displacement diagram of the cracked ductile specimen (W_1) and to equate it with the area under the linear load-displacement graph of the virtual cracked brittle sample (W_2) (see Fig. 10). In this

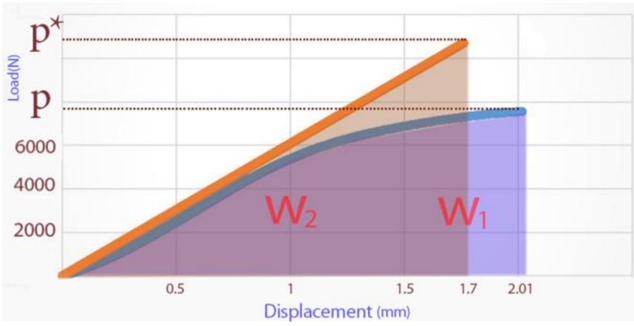

Fig. 10 The concept of determining the equivalent fracture load

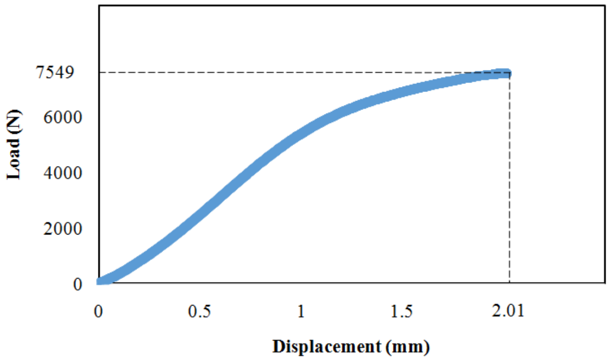

Fig. 11 Average load-displacement curve of the cracked specimens made of Al7075-T6

case, it should only be noticed that the gradients of the graphs are the same. In this way, the fracture load of the equivalent brittle cracked specimen (p^*) is ascertained. Then, this load should be applied as the LCC of the cracked specimen to the FE model, and the mode I stress intensity factor (SIF) obtained is equal to K_{Ic}^*.

5. Results and discussion

As previously stated, in order to examine ductile fracture by combining EMC with the brittle fracture criteria of PS and MS, it is necessary to calculate the critical distance of r_c, which, according to Eq. (10), needs the values of K_{Ic}^* (equivalent fracture toughness) and σ_f^* (equivalent tensile strength). For calculating σ_f^* according to the simple procedure prescribed in Ref. (Torabi, Kalantari, *et al.* 2018), the area below the true stress-strain graph shown in Fig. 2 is first calculated up to the ultimate strength point, which is numerically obtained equal to 38.74 MPa. Then, by assuming that the area below the linear stress-strain curve of the equivalent material with the slope (elastic modulus) of 72 GPa for Al7075-T6, which is actually a triangle, is also equal to 38.74 MPa, the value of σ_f^* for this material is specified as 2362 MPa.

To determine the equivalent fracture toughness, pure mode I fracture tests are performed on five cracked specimens. These tests are performed using the loading fixture utilized in the present study to perform the fracture experiments of U-notched samples and in accordance with the conditions detailed in Ref. (Ayatollahi and Saboori 2015). The cracked samples are cut by a wire-cut machine.

Table 3 The properties obtained for the virtual elastic material equivalent to the tested Al7075-T6

Material Property	Value
Equivalent tensile strength, σ_f^* [MPa]	2362
Equivalent fracture toughness, K_{Ic}^* [MPa√m]	64.75
The critical distance of r_c [mm]	0.12
The critical distance of d_c [mm]	0.48

A wire of 0.2 mm diameter is applied to introduce cracks to the samples. From the average of the results of the fracture test of the cracked samples, the related load-displacement diagram is obtained as Fig. 11.

According to the results of the fracture tests, the average LCC of the tested cracked specimens is about 7549 N. To determine the fracture load of the equivalent elastic material in accordance with the method depicted in Fig. 10, the area below the load-displacement curve of the ductile material should be calculated, which is obtained to be equal to W = 9.43 J. Then, a straight line tangent to the elastic-plastic diagram of Fig. 11 is drawn and is extended to the point where the area below it is equal to 9.43 J. In this way, the LCC of the virtual linear elastic cracked specimen is obtained equal to 10714 N. After applying this load to the linear elastic FE model of the cracked sample, the mode I critical stress intensity factor, which is the equivalent fracture toughness (K_{Ic}^*), is determined equal to 64.75 MPa√m.

Using the values obtained for K_{Ic}^* and σ_f^*, based on Eq. (10), the value of r_c is 0.12 mm. Given the value of r_c, the value of the critical distance d_c, which is required in the MS criterion, is also specified as $d_c = 4r_c = 0.48$ mm.

Now that the properties of the virtual elastic material equivalent to the tested Al7075-T6 are known (listed in Table 3), the PS and MS criteria relations can be exploited to predict the results of the mixed mode I/III fracture tests conducted on the U-notched Al7075-T6 specimens. In this regard, the critical values of the NSIFs due to the critical loads reported in Table 2 should be obtained. After determining the values of the normal and out-of-plane shear stresses at the notch tip, the NSIFs can be calculated for U-notch by means of the following relations (Saboori *et al.* 2017):

$$K_I^{U,\rho} = \sqrt{2\pi r_0}\,\frac{\sigma_{\theta\theta}(r_0,0)}{1+\omega_1} \tag{11}$$

$$K_{III}^{U,\rho} = \sqrt{2\pi r_0}\,\frac{\sigma_{z\theta}(r_0,0)}{1+(r_0/r_3)^{\mu_3-1/2}} \tag{12}$$

where the values of the constant parameters ω_1, μ_3, and r_3 have been given in Ref. (Saboori *et al.* 2016). As depicted in Fig. 8, r_0 is the distance between the origins of the notch coordinate systems and the notch tip.

In view of the relative geometric complexity of the utilized test configuration, the values of the stresses $\sigma_{\theta\theta}$ and $\sigma_{z\theta}$ at the notch tip that exist in the above equations

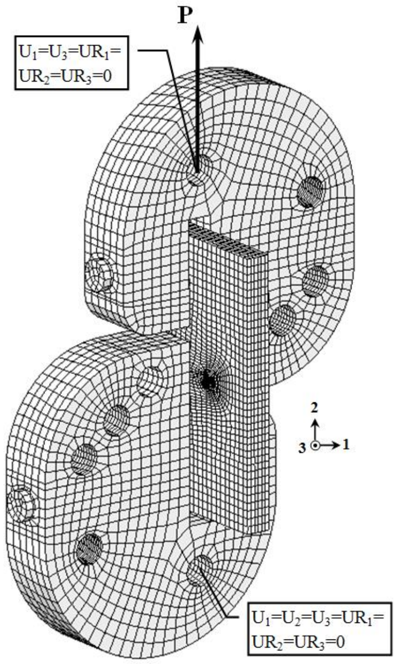

Fig. 12 A view of the FE model of the employed fracture test configuration

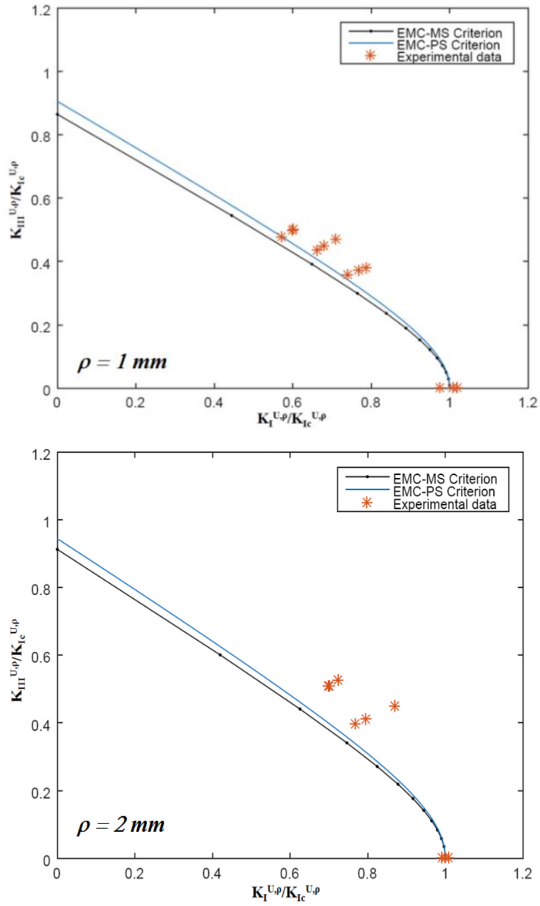

Fig. 13 The predictions of the EMC-PS and EMC-MS criteria for fracture limit of the U-notched Al-7075-T6 samples with notch tip radii of 1 and 2 mm along with the test results

must be computed by means of the finite element analysis. For this purpose, the FE simulation of the mixed mode I/III test configuration is performed using a commercially available software for the notches with two different tip radii. By applying the LCC of the test samples to the FE model and performing linear elastic analysis, the values of normal stress and out-of-plane shear stress are computed. As seen in Fig. 12, the FE model is constructed to include the meshed models of both the fixture sections, the test specimen, and the bolts connecting the sample to the fixture. The loading fixture and the connecting bolts are simulated as rigid bodies. 20-node quadratic brick elements are used to mesh the test specimen model. The finer elements are considered at the notch tip and its proximity due to the high stress gradient. The manner of applying the load and boundary conditions defined in accordance with the actual conditions in the case of pure mode I loading is also observed in Fig. 12. Given the steel material of the fixture and the fastening bolts and the aluminum material of the test specimen, a friction coefficient of 0.47 (Ashby 2005) is defined for surface-to-surface contact between the fixture and the specimen, as well as between the specimen and the fastening bolts. Other details of the FE simulation can be found in Ref. (Saboori *et al.* 2017).

Comparison of the experimental results with the predictions of EMC-PS and EMC-MS combined criteria in the mixed mode I/III loading case is performed in the form of the fracture limit diagrams. For both of these criteria, the graphs are plotted as dimensionless normalized parameter of $K_{III}^{U,\rho}/K_{Ic}^{U,\rho}$ versus $K_{I}^{U,\rho}/K_{Ic}^{U,\rho}$. The mixed mode I/III fracture curves of the U-notched Al7075-T6 samples with ρ = 1 and 2 mm are plotted in Fig. 13 using the EMC-PS and EMC-MS criteria. The results of the conducted fracture tests are also illustrated in this figure. It is observed that for almost all radii of the notch tip and the loading modes considered, the results of the three repetitive tests are very close together, conveying that the construction and fracture testing of the specimens have been carried out with high precision.

One of the things evident in Fig. 13 is that the EMC-MS and EMC-PS criteria provide very close predictions for both the notches with ρ = 1 and 2 mm. Fig. 13 also indicates that these two criteria predict the results of the conducted fracture tests with good accuracy. In order to quantitatively compare the theoretical and the test results obtained in different loading modes, one can use a parameter, called the normalized effective NSIF (NENSIF), $K_{eff}^{U,\rho}$, which is defined by the following equation:

$$K_{eff}^{U,\rho} = \sqrt{\left(\frac{K_{I}^{U,\rho}}{K_{Ic}^{U,\rho}}\right)^2 + \left(\frac{K_{III}^{U,\rho}}{K_{Ic}^{U,\rho}}\right)^2} \quad (13)$$

The experimental values of $K_{eff}^{U,\rho}$, as well as the corresponding theoretical values, are listed in Table 4. The percentage difference between the theoretical and experimental values of NENSIF is also given in this table.

The difference between the theoretical estimations and the experimental results of Table 4 also confirms that both

Table 4 The theoretical and experimental values of $K_{eff}^{U,\rho}$ for mixed-mode I/III fracture of Al-7075-T6 U-notched specimens

ρ (mm)	loading mode, β (°)	Mean Exp. value	EMC-PS criterion		EMC-MS criterion	
			Predicted value	discrepancy (%)	Predicted value	discrepancy (%)
1	0	1.00	1.00	0	1.00	0
	40	0.85	0.82	3	0.80	5
	65	0.82	0.78	4	0.75	7
	72	0.77	0.76	1	0.72	5
				Avg.: 2.0		**Avg.: 4.2**
2	0	1.00	1.00	0	1.00	0
	40	0.91	0.85	6	0.81	10
	65	0.87	0.79	8	0.77	10
				Avg.: 4.6		**Avg.: 6.6**
				Total Avg.: 3.3		**Total Avg.: 5.4**

the EMC-MS and EMC-PS criteria have a very good precision in the fracture study of the U-notched Al7075-T6 samples under mixed mode I/III loading. As can be seen, the average percentage difference between the theoretical predictions and the results of the experiments related to the various tip radii and loading modes is 3.3% for the EMC-PS criterion and 5.4% for EMC-MS one.

One of the reasons for the difference between the experimental and theoretical results can be the stress field used in the EMC-MS and EMC-PS criteria, because it satisfies the boundary conditions only on the limited points of the notch edge (not on the entire edge). Another reason for the difference may be the error of the carried out experiments. For example, one of the laboratory errors can be related to the error of the testing machine in measuring the specimens LCC. Of course, it should be noted that in order to minimize the error of the laboratory results, the fracture test of each specimen is repeated three times, but still there may be some errors in the laboratory results. The other reason for the difference between the theoretical and experimental results can be related to the lags between the parts of the mixed mode I/III loading fixture, as well as those between the fixture and the test sample.

In Table 4, it can be seen that using the EMC-PS criterion, there is less difference between the theoretical and experimental results compared to EMC-MS criterion, and the EMC-PS criterion for both ρ = 1 and 2 mm provides better predictions than the EMC-MS one. However, because of the small discrepancies between the two criteria, one can say that none of them has a significant superiority to the other, and both criteria provide accurate predictions. Nonetheless, according to Fig. 13, with increasing of the contribution of Mode III in the mixed mode I/III loading, the discrepancy between the two criteria grows a little. In addition, the deviation between the curves of these two criteria decreases with increasing the radius of the notch tip. Another point understood from Table 4 is that both the EMC-MS and EMC-PS criteria estimate the fracture resistance of the notched samples with a smaller notch tip radius with greater accuracy. This is due to the fact that the accuracy of the closed-form relation of the stress distribution used in the formulation of these criteria is greater for notches with a larger ratio of the notch depth/notch radius (Torabi and Alaei 2016). Since the notch depth in all of the notched specimens of the present study is considered to be 30 mm and constant, in the case of samples with a smaller notch tip radius, the accuracy of the relation of the stress distribution is higher. As a result, the prediction of the theoretical criteria is more consistent with the experimental results in those cases. On the other hand, given that the curves of EMC-MS criterion are lower than those of EMC-PS criterion in Fig. 13, the safe region estimated by EMC-MS criterion is smaller than that by EMC-PS criterion, and therefore, EMC-MS is more conservative.

Finally, it should be mentioned that mode III and mode II deformations in cracked and notched components mostly occur dependently along the component thickness. This is known as three-dimensional (3D) effects which can influence fracture behavior of notched specimens subjected to the spatial loading conditions such as mixed mode I/III loading. In particular, Pook and his collaborators have shown in the recent contributions (Pook 2013; Pook *et al.* 2017; Pook *et al.* 2016) that the application of nominal mode III to cracked or notched components gives rise to coupled mode II loading and vice versa, which could be even higher and more critical than the nominal applied load, especially at the free surfaces. As mentioned earlier, the PS and the MS failure models have been extended to the general loading conditions of mixed mode I/II/III (Saboori *et al.* 2016) and therefore, the EMC-PS and EMC-MS criteria are capable to investigate the fracture of notched ductile materials considering the 3D effects.

As noted earlier, in the present paper, it is the first time that the validation of the results of applying the EMC in the study of the failure of notched ductile materials under mixed mode loading involving out-of-plane shear is examined. But the validity of the results of using the EMC in in-plane mixed mode loading conditions has already been shown for various geometries, many of which are mentioned in the Introduction section. Since the EMC is investigated here for the first time in the case of out-of-plane loading, relatively finite geometries and loading modes are studied including U-notches with 1 and 2 mm notch tip radii and a maximum of three mixed loading modes in addition to pure mode I. In the future, however, the performance of EMC in the presence of out-of-plane load for other notch geometries will also be evaluated by the authors.

6. Conclusions

In this study, the ductile fracture of aluminum plates of Al7075-T6 containing U-notches was investigated experimentally and theoretically under out-of-plane mixed mode I/III loading conditions. A new experimental campaign was proposed and carried out in this regard. To perform the fracture tests under combined tension/out-of-plane shear loading, a previously-developed loading fixture was employed that enables the creation of a variety of loading modes from pure mode I to pure mode III. To predict the fracture of the U-notched Al7075-T6 specimens, the combination of two stress-based fracture criteria, i.e. the point stress (PS) and mean stress (MS) criteria, with the Equivalent Material Concept (EMC) was used. The well-matched theoretical predictions and experimental results revealed that the use of the combination of EMC with the MS and PS brittle fracture criteria (referred to as the EMC-MS and EMC-PS criteria) has been successful to study the fracture of U-notched Al7075-T6 components under mixed mode I/III loading. Although EMC-PS criterion provided relatively more accurate predictions than EMC-MS one, this difference is not noticeable. It was also observed that the predictions of EMC-MS criterion were more conservative than those of EMC-PS criterion. The results indicated that under mixed mode I/III loading conditions, the difference between the EMC-MS and EMC-PS criteria grows a little by increasing the contribution of mode III loading. Meanwhile, with increasing the notch tip radius, the discrepancy between the fracture limit curves of EMC-MS and EMC-PS criteria was found diminishing.

References

Ashby, M.F. (2005), *Materials Selection in Mechanical Design*, MRS Bull.

ASTM B646-19 (2019), *Standard Practice for Fracture Toughness Testing of Aluminum Alloys*, ASTM International; West Conshohocken, PA.

ASTM E8 / E8M-16a (2016), *Standard Test Methods for Tension Testing of Metallic Materials*, ASTM International; West Conshohocken, PA.

Ayatollahi, M.R. and Saboori, B. (2015), "A new fixture for fracture tests under mixed mode I/III loading", *European J. Mech. A/Solids*, **51**(0), 67-76. https://doi.org/10.1016/j.euromechsol.2014.09.012.

Ayatollahi, M.R. and Torabi, A.R. (2010a), "Brittle fracture in rounded-tip V-shaped notches", *Mater. Design* **31**(1), 60-67. https://doi.org/10.1016/j.matdes.2009.07.017.

Ayatollahi, M.R. and Torabi, A.R. (2010b), "Investigation of mixed mode brittle fracture in rounded-tip V-notched components", *Eng. Fracture Mech.*, **77**(16), 3087-3104. https://doi.org/10.1016/j.engfracmech.2010.07.019.

Cicero, S., Torabi, A.R., Madrazo, V. and Azizi, P. (2018), "Prediction of fracture loads in PMMA U-notched specimens using the equivalent material concept and the theory of critical distances combined criterion", *Fatigue Fracture Eng. Maer. Struct.*, **41**(3), 688-699. https://doi.org/10.1111/ffe.12728.

El Minor, H., Pluvinage, G. and Azari, Z. (2007), "An elliptical fracture criterion for mixed mode fracture I+ II emanating from notches", *Struct. Eng. Mech.*, **26**(1), 87-97. https://doi.org/10.12989/sem.2007.26.1.087.

Erdogan, F. and Sih, G.C. (1963), "On the Crack Extension in Plates Under Plane Loading and Transverse Shear", *J. Basic Eng.*, **85**(4), 519-525. https://doi.org/10.1115/1.3656897.

Fuentes, J.D., Cicero, S., Berto, F., Torabi, A.R., Madrazo, V. and Azizi, P. (2018), "Estimation of Fracture Loads in AL7075-T651 Notched Specimens Using the Equivalent Material Concept Combined with the Strain Energy Density Criterion and with the Theory of Critical Distances", *Metals*, **8**(2), 87. https://doi.org/10.3390/met8020087.

Glinka, G. (1985), "Energy density approach to calculation of inelastic strain-stress near notches and cracks", *Eng. Fracture Mech.*, **22**(3), 485-508. https://doi.org/10.1016/0013-7944(85)90148-1.

Gómez, F.J., Elices, M., Berto, F. and Lazzarin, P. (2007), "Local strain energy to assess the static failure of U-notches in plates under mixed mode loading", *J. Fracture* **145**(1), 29-45. https://doi.org/10.1007/s10704-007-9104-3.

Gómez, F.J., Elices, M., Berto, F. and Lazzarin, P. (2008), "A generalised notch stress intensity factor for U-notched components loaded under mixed mode", *Eng. Fracture Mech.*, **75**(16), 4819-4833. http://doi.org/10.1016/j.engfracmech.2008.07.001.

Gómez, F.J., Elices, M., Berto, F. and Lazzarin, P. (2009), "Fracture of V-notched specimens under mixed mode (I + II) loading in brittle materials", *J. Fracture* **159**(2), 121-135. https://doi.org/10.1007/s10704-009-9387-7.

Haeri, H., Sarfarazi, V. and Zhu, Z. (2018), "PFC3D simulation of the effect of particle size on the single edge-notched rectangle bar in bending test", *Struct. Eng. Mech.*, **68**(4), 497-505. https://doi.org/10.12989/sem.2018.68.4.497.

Lee, K.-L. (2010), "Mechanical behavior and buckling failure of sharp-notched circular tubes under cyclic bending", *Struct. Eng. Mech.*, **34**(3), 367-376. https://doi.org/10.12989/sem.2010.34.3.367.

Lee, K.-L., Chang, K.-H. and Pan, W.-F. (2016), "Failure life estimation of sharp-notched circular tubes with different notch depths under cyclic bending", *Struct. Eng. Mech.*, **60**(3), 387-404. https://doi.org/10.12989/sem.2016.60.3.387.

Molski, K. and Glinka, G. (1981), "A method of elastic-plastic stress and strain calculation at a notch root", *Mater. Sci. Eng.*, **50**(1), 93-100. https://doi.org/10.1016/0025-5416(81)90089-6.

Pook, L. (2013), "A 50-year retrospective review of three-dimensional effects at cracks and sharp notches", *Fatigue Fracture Eng. Maer. Struct.*, **36**(8), 699–723. https://doi.org/10.1111/ffe.12074.

Pook, L.P., Berto, F. and Campagnolo, A. (2017), "State of the art of corner point singularities under in-plane and out-of-plane loading", *Eng. Fracture Mech.*, **174**, 2-9. https://doi.org/10.1016/j.engfracmech.2016.10.001.

Pook, L.P., Campagnolo, A. and Berto, F. (2016), "Coupled fracture modes of discs and plates under anti-plane loading and a disc under in-plane shear loading", *Fatigue Fracture Eng. Maer. Struct.*, **39**(8), 924-938. https://doi.org/10.1111/ffe.12389.

Saboori, B., Ayatollahi, M.R., Torabi, A.R. and Berto, F. (2016), "Mixed mode I/III brittle fracture in round-tip V-notches", *Theoretical Appl. Fracture Mech.*, **83**, 135-151. https://doi.org/10.1016/j.tafmec.2015.12.002.

Saboori, B., Torabi, A., Berto, F. and Razavi, S. (2018), "Averaged strain energy density to assess mixed mode I/III fracture of U-notched GPPS samples", *Struct. Eng. Mech.*, **65**(6), 699-706.

https://doi.org/10.12989/sem.2018.65.6.699.

Saboori, B., Torabi, A.R., Ayatollahi, M.R. and Berto, F. (2017), "Experimental verification of two stress-based criteria for mixed mode I/III brittle fracture assessment of U-notched components", *Eng. Fracture Mech.*, **182**, 229-244. https://doi.org/10.1016/j.engfracmech.2017.06.005.

Saboori, B., Torabi, A.R. and Keshavarz Mohammadian, S. (2018), "Experimental and stress-based theoretical studies on mixed mode I/III fracture of round-tip V-notched Polystyrene specimens", *Theoretical Appl. Fracture Mech.*, **95**, 283-305. https://doi.org/10.1016/j.tafmec.2018.03.008.

Sapora, A. and Firrao, D. (2017), "Finite fracture mechanics predictions on the apparent fracture toughness of as-quenched Charpy V-type AISI 4340 steel specimens", *Fatigue Fracture Eng. Maer. Struct.*, **40**(6), 949-958. https://doi.org/10.1111/ffe.12555.

Sarfarazi, V., Haeri, H., Ebneabbasi, P. and Bagheri, K. (2019), "Simulation of the tensile behaviour of layered anisotropy rocks consisting internal notch", *Struct. Eng. Mech.*, **69**(1), 51-67. https://doi.org/10.12989/sem.2018.69.1.051.

Seweryn, A. (1994), "Brittle fracture criterion for structures with sharp notches", *Eng. Fracture Mech.*, **47**(5), 673-681. https://doi.org/10.1016/0013-7944(94)90158-9.

Susmel, L. and Taylor, D. (2008), "The theory of critical distances to predict static strength of notched brittle components subjected to mixed-mode loading", *Eng. Fracture Mech.*, **75**(3), 534-550. https://doi.org/10.1016/j.engfracmech.2007.03.035.

Torabi, A. and Alaei, M. (2016), "Application of the equivalent material concept to ductile failure prediction of blunt V-notches encountering moderate-scale yielding", *J. Damage Mech.*, **25**, 853-877. https://doi.org/10.1177/1056789515625451.

Torabi, A. and Berto, F. (2014), "Mixed mode fracture assessment of U-notched graphite Brazilian disk specimens by means of the local energy", *Struct. Eng. Mech.*, **50**(6), 723-740. https://doi.org/10.12989/sem.2014.50.6.723.

Torabi, A.R. (2012a), "Estimation of tensile load-bearing capacity of ductile metallic materials weakened by a V-notch: The equivalent material concept", *Mater. Sci. Eng. A*, **536**, 249-255. https://doi.org/10.1016/j.msea.2012.01.007.

Torabi, A.R. (2012b), "On the use of the equivalent material concept to predict tensile load-bearing capacity of ductile steel bolts containing V-shaped threads", *Eng. Fracture Mech.*, **97**, 136-147. https://doi.org/10.1016/j.engfracmech.2012.10.021.

Torabi, A.R. (2013), "Ultimate bending strength evaluation of U-notched ductile steel samples under large-scale yielding conditions", *J. Fracture* **180**, 261-268. https://doi.org/10.1007/s10704-013-9804-9.

Torabi, A.R. and Alaei, M. (2015), "Mixed-mode ductile failure analysis of V-notched Al 7075-T6 thin sheets", *Eng. Fracture Mech.*, **150**, 70-95. https://doi.org/10.1016/j.engfracmech.2015.10.037.

Torabi, A.R., Berto, F., Campagnolo, A. and Akbardoost, J. (2017), "Averaged strain energy density criterion to predict ductile failure of U-notched Al 6061-T6 plates under mixed mode loading", *Theoretical Appl. Fracture Mech.*, **91**, 86-93. https://doi.org/10.1016/j.tafmec.2017.04.010.

Torabi, A.R., Berto, F. and Razavi, S.M.J. (2018), "Ductile failure prediction of thin notched aluminum plates subjected to combined tension-shear loading", *Theoretical Appl. Fracture Mech.*, **97**, 280-288. https://doi.org/10.1016/j.tafmec.2017.05.003.

Torabi, A.R., Berto, F. and Sapora, A. (2019), "Finite fracture mechanics assessment in moderate and large scale yielding regimes", *Metals*, **9**(5), 602. https://doi.org/10.3390/met9050602.

Torabi, A.R., Campagnolo, A. and Berto, F. (2016a), "Mixed mode I/II crack initiation from U-notches in Al 7075-T6 thin plates by large-scale yielding regime", *Theoretical Appl. Fracture Mech.*, **86**, 284-291. https://doi.org/10.1016/j.tafmec.2016.08.002.

Torabi, A.R., Campagnolo, A. and Berto, F. (2016b), "A successful combination of the equivalent material concept and the averaged strain energy density criterion for predicting crack initiation from blunt V-notches in ductile aluminum plates under mixed mode loading", *Physical Mesomechanics*, **19**, 382-391. https://doi.org/10.1134/S1029959916040056.

Torabi, A.R., Campagnolo, A. and Berto, F. (2017), "Large-Scale Yielding Failure Prediction of Notched Ductile Plates by Means of the Linear Elastic Notch Fracture Mechanics", *Strength Mater.*, **49**(2), 224–233. https://doi.org/10.1007/s11223-017-9861-9.

Torabi, A.R. and Habibi, R. (2016), "Investigation of ductile rupture in U-notched Al 6061-T6 plates under mixed mode loading", *Fatigue Fracture Eng. Mater Struct.*, **39**, 551-565. https://doi.org/10.1111/ffe.12376.

Torabi, A.R., Kalantari, M.H. and Aliha, M.R.M. (2018), "Fracture analysis of dissimilar Al-Al friction stir welded joints under tensile/shear loading", *Fatigue Fracture Eng. Maer. Struct.*, **41**(9), 2040-2053. https://doi.org/10.1111/ffe.12841.

Torabi, A.R. and Kamyab, M. (2019a), "The fictitious material concept", *Eng. Fracture Mech.*, **209**, 17-31. https://doi.org/10.1016/j.engfracmech.2019.01.022.

Torabi, A.R. and Kamyab, M. (2019b), "Mixed mode I/II failure prediction of thin U-notched ductile steel plates with significant strain-hardening and large strain-to-failure: The Fictitious Material Concept", *European J. Mech. A/Solids*, **75**, 225-236. https://doi.org/10.1016/j.euromechsol.2019.02.004.

Torabi, A.R. and Kamyab, M. (2019c), "Notch ductile failure with significant strain-hardening: The modified equivalent material concept", *Fatigue Fracture Eng. Maer. Struct.*, **42**(2), 439-453. https://doi.org/10.1111/ffe.12921.

Torabi, A.R. and Keshavarzian, M. (2016), "Evaluation of the load-carrying capacity of notched ductile plates under mixed mode loading", *Theoretical Appl. Fracture Mech.*, **85**, 375-386. https://doi.org/10.1016/j.tafmec.2016.04.009.

Torabi, A.R. and Mohammad Hosseini, B. (2017), "Large plasticity induced crack initiation from U-notches in thin aluminum sheets under mixed mode loading", *Eng. Solid Mech.*, **5**(1), 39-60. https://doi.org/10.5267/j.esm.2016.10.001.

Torabi, A.R., Rahimi, A.S. and Ayatollahi, M.R. (2018), "Fracture study of a ductile polymer-based nanocomposite weakened by blunt V-notches under mode I loading: Application of the Equivalent Material Concept", *Theoretical Appl. Fracture Mech.*, **94**, 26-33. https://doi.org/10.1016/j.tafmec.2018.01.002.

Torabi, A.R. and Saboori, B. (2018), "Experimental and theoretical investigation of mixed mode I/III brittle fracture of U-notched polystyrene components", *J. Strain Analysis for Eng. Design*, **53**(1), 15-25. https://doi.org/10.1177/0309324717739725.

Torabi, A.R., Saboori, B., Mohammadian, S.K. and Ayatollahi, M.R. (2018), "Brittle failure of PMMA in the presence of blunt V-notches under combined tension-tear loading: Experiments and stress-based theories", *Polym. Testing*, **72**, 94-109. https://doi.org/10.1016/j.polymertesting.2018.10.002.

Wieghardt, K., Sommerfeld, A. and Rossmanith, H. (1995), "On splitting and cracking of elastic bodies", *Fatigue Fracture Eng. Maer. Struct.*, **18**(12), 1371-1405. https://doi.org/10.1111/j.1460-2695.1995.tb00864.x.

CC